

Nucleon structure: from electromagnetic Form Factors to Generalized Parton Distributions

Mostafa Hoballah on behalf of all contributors

AG GDR QCD
Strasbourg, 27-29 September 2023



Moments of the proton charge density

M. Atoui, M.B. Barbaro, M. Hoballah, C. Keyrouz, M. Lassaut, D. Marchand,
G. Quéméner, E.Voutier, R. Kunne, J. Van De Wiele

M. Hoballah *et al.* Phys . Let. B 808 135669 (2020)

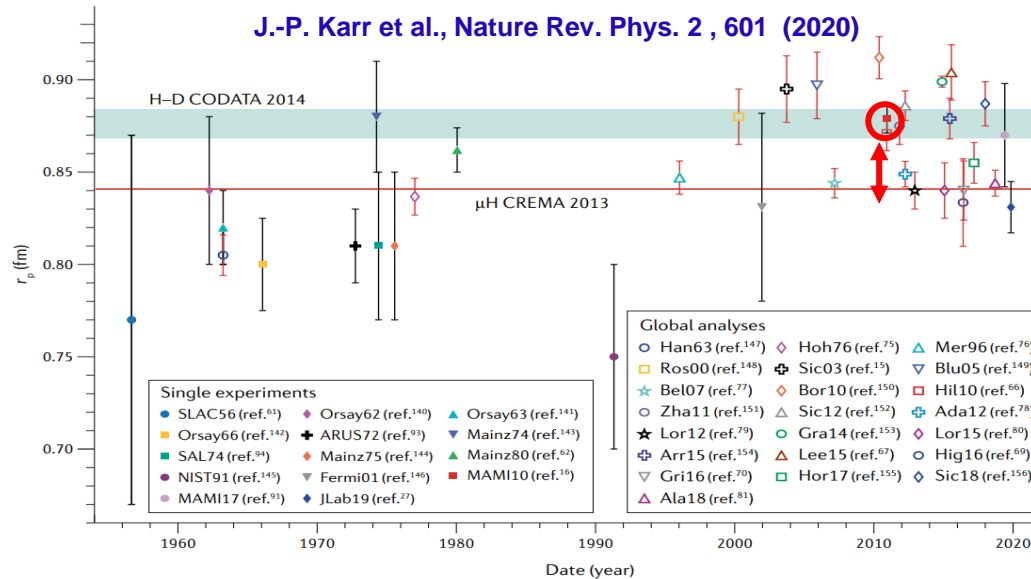
M. Atoui *et al.*, ArXiv:2304.1352 [nucl-ex]



Disclaimer: all slides on this topic are taken from M. Atoui, with her permission.



Moments of the proton charge density: Context



Subject no longer under pressure
(CODATA 2018 average)
but
discrepancies not fully understood

$$\frac{d\sigma}{d\Omega} = \frac{d\sigma}{d\Omega} \Big|_{\text{Mott}} \times \left[\frac{G_E^2(k^2) + \tau G_M^2(k^2)}{1 + \tau} + 2\tau \tan^2\left(\frac{\theta}{2}\right) G_M^2(k^2) \right]$$

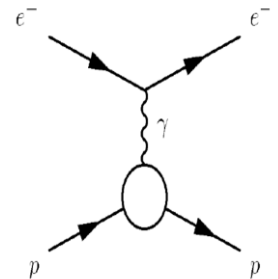
The **radius** is defined as

$$r_p = \sqrt{-6 \frac{\partial G_E^2(k^2)}{\partial k^2} \Big|_{k^2=0}}$$

Issues faced when evaluating the radius:

- What is the best k^2 range to fit and extrapolate the Form Factor?
- What function to use? **Model assumption of the functional behavior** of the form factor
- **Sensitivity** to variations of the Form Factor at low k^2

Goal: Another method to evaluate the moments of the charge density from experimental data





The integral method

- **Spatial density** $\rho_E(\mathbf{r}) = \frac{1}{(2\pi)^3} \int_{R^3} d^3\mathbf{k} e^{i\mathbf{k}\mathbf{r}} \mathbf{G}_E(\mathbf{k})$
- **Moments** $(r^\lambda, \rho_E) = \int d^3\mathbf{r} r^\lambda \rho_E(\mathbf{r})$

Non relativistic approach; Breit Frame

$$(r^\lambda, \rho_E) = \frac{1}{2\pi^3} \int_{R^3} d^3\mathbf{k} \mathbf{G}_E(\mathbf{k}) \int_{R^3} d^3\mathbf{r} e^{i\mathbf{k}\mathbf{r}} r^\lambda$$

Finite term

Divergent term needs to be regularized as by definition the moment r^λ is finite

$$g_\lambda(k) = \int_{R^3} d^3r e^{i\mathbf{k}\mathbf{r}} r^\lambda$$

can be taken as the limit of the convergent integral

$$g_\lambda(k) = \lim_{\epsilon \rightarrow 0^+} \int_{R^3} d^3r e^{-\epsilon r} e^{i\mathbf{k}\mathbf{r}} r^\lambda = \lim_{\epsilon \rightarrow 0^+} I_\lambda(k, \epsilon)$$

- **Moments r^λ can be written as:** $(r^\lambda, \rho_E) = \frac{2}{\pi} \Gamma(\lambda + 2) \lim_{\epsilon \rightarrow 0^+} \int_0^\infty dk \mathbf{G}_E(k) \frac{k \sin \left[(\lambda+2) \text{Arctan} \left(\frac{k}{\epsilon} \right) \right]}{(k^2 + \epsilon^2)^{\frac{\lambda}{2} + 1}}$

Condition: $\lambda > -3$

- **Integer λ :** $(r^m, \rho_E) = \frac{2}{\pi} (m + 1)! \lim_{\epsilon \rightarrow 0^+} \epsilon^{m+2} \int_0^\infty dk \mathbf{G}_E(k) \frac{k}{(k^2 + \epsilon^2)^{m+2}} \Phi_m \left(\frac{k}{\epsilon} \right)$ with $\Phi_m \left(\frac{k}{\epsilon} \right) = \sum_{j=0}^{m+2} \sin \left(\frac{j\pi}{2} \right) \frac{(m+2)!}{j!(m+2-j)!} \left(\frac{k}{\epsilon} \right)^j$

For even order moments : IM recovers formally the same quantities as the derivative



The integral method: what do we gain?

- Odd moments can now be accessed directly (Can even access fractional moments!)
- No change in the extracted value for even moments, but:
 - Conceptual change residing in the fact that doing integrals rather than derivatives , implies that all Q^2 range should be considered for the determination of the FF, no truncation in the FF data fit.
- Less sensitive to form factor variations
- Emphasis on:
 - Measurements of FFs at **low Q^2 (long range effects)** as well as **high Q^2 (short range effects)** are equally important for the study of nucleon structure

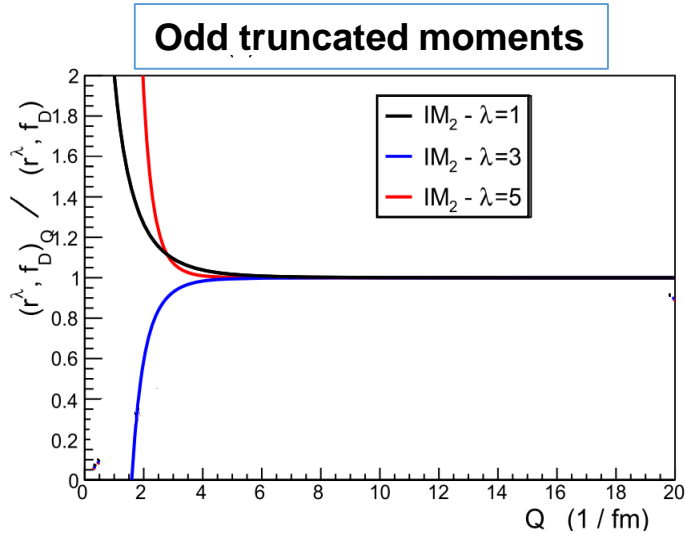


Application of the method

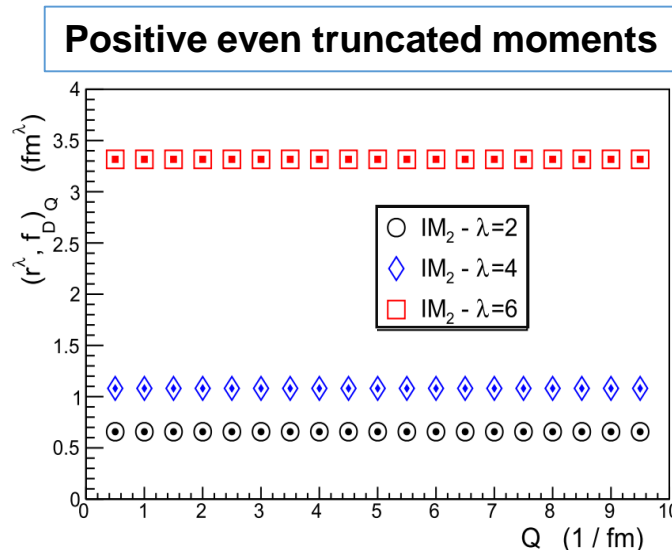
Experimental measurements of the Form Factor do not extend to infinite k^2 :

- **But:** Integrals are most likely to saturate at a squared four-momentum transfer value well below infinity.
- **Hence:** **Cut-off Q** replaces the infinite integral boundary : **truncated moments**.

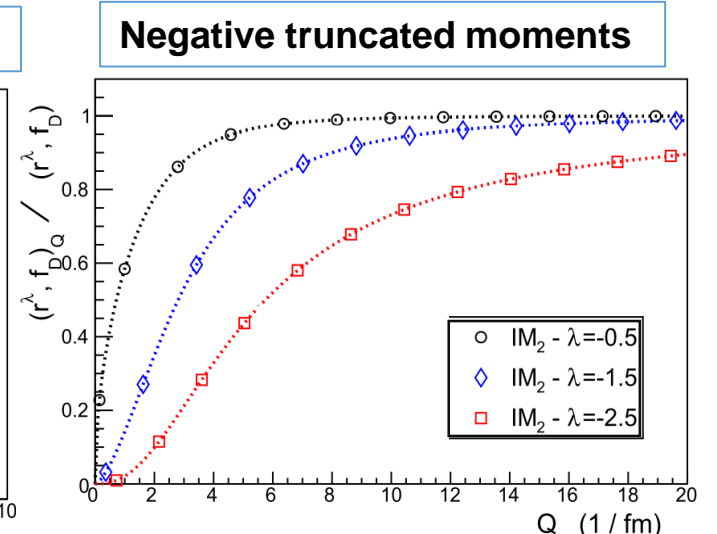
Use the polynomial ratio parametrization $G_E(k) = \frac{1+a_1k^2}{1+b_1k^2+b_2k^4+b_3k^6}$ J.J. Kelly, Phys. Rev. C 70 (2004) 068202.



The method rapidly saturates about 6 fm^{-1} , in a momentum region well covered by proton electromagnetic FF data.



Q-independence is reproduced



Convergence is not guaranteed within the domain covered by experimental data



Application to experimental data

- Select G_E from elastic electron scattering experiments

- **Rosenbluth Separation** : Measure σ_R at a fixed k^2

for different values of beam energy and scattering angle

- **G_M contribution is strongly suppressed**: at very low k^2

→ 21 data sets:

$$[2.15 \times 10^{-4} \text{GeV}^2] \quad 5.51 \times 10^{-3} \leq k^2 (\text{fm}^{-2}) \leq 226 [8.8 \text{ GeV}^2]$$

- Fit simultaneously the different datasets using the functional form

$$G_E(k) = \eta_i \frac{1 + a_1 k^2}{1 + b_1 k^2 + b_2 k^4 + b_3 k^6}$$

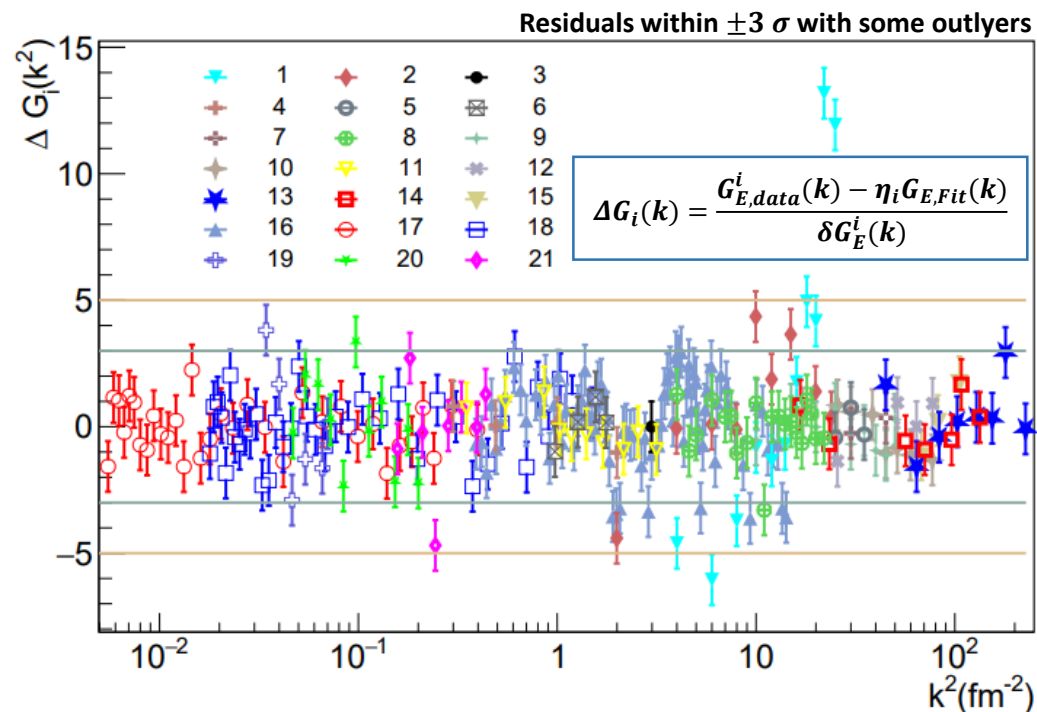
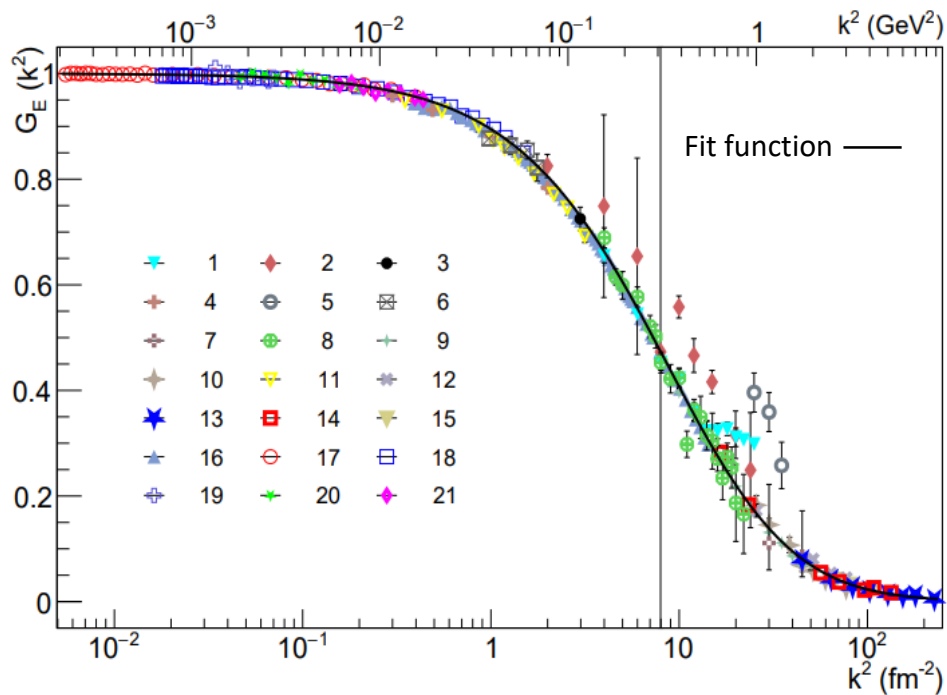
- The **same functional behavior** is assumed for each dataset

- A **separate normalization parameter η_i** is considered for each dataset number i

Data Set Number	Year	Author	Number of data	k^2 -range	
				k_{min}^2 (fm ⁻²)	k_{max}^2 (fm ⁻²)
1	1961	Bumiller <i>et al.</i>	11	4.00	25.0
2	1961	Littauer <i>et al.</i>	9	2.00	24.0
3	1962	Lehmann <i>et al.</i>	1	2.98	2.98
4	1963	Dudelzak <i>et al.</i>	4	0.30	2.00
5	1963	Berkelman <i>et al.</i>	3	25.0	35.0
6	1966	Frèrejacque <i>et al.</i>	4	0.98	1.76
7	1966	Chen <i>et al.</i>	2	30.0	45.0
8	1966	Janssens <i>et al.</i>	20	4.00	22.0
9	1971	Berger <i>et al.</i>	9	1.00	50.0
10	1973	Bartel <i>et al.</i>	8	17.2	77.0
11	1975	Borkowski <i>et al.</i>	10	0.35	3.15
12	1994	Walker <i>et al.</i>	4	25.7	77.0
13	1994	Andivahis <i>et al.</i>	8	44.9	226.
14	2004	Christy <i>et al.</i>	7	16.7	133.
15	2005	Qattan <i>et al.</i>	3	67.8	105.
16	2014	Bernaer <i>et al.</i>	77	0.39	14.2
17	2019	Xiong <i>et al.</i> - 1.1 GeV	33	5.51×10^{-3}	3.96×10^{-1}
18	2019	Xiong <i>et al.</i> - 2.1 GeV	38	1.79×10^{-2}	1.49
19	2021	Mihovilović <i>et al.</i> - 195 MeV	6	3.43×10^{-2}	6.99×10^{-2}
20	2021	Mihovilović <i>et al.</i> - 330 MeV	11	4.69×10^{-2}	2.00×10^{-1}
21	2021	Mihovilović <i>et al.</i> - 495 MeV	8	1.57×10^{-1}	4.37×10^{-1}



Fit results



	a_1 [10^{-1} fm^2]	b_1 [10^{-1} fm^2]	b_2 [10^{-1} fm^4]	b_3 [10^{-3} fm^6]
	8.8030	9.9402	1.0454	2.7020
Statistical errors	0.0012	0.0025	0.0013	0.0153
Systematic errors	0.0096	0.0019	0.0031	0.0317

- Normalization parameters η_i**
- Recent experiments (2010-2021): Deviation from unity is smaller than 1%
 - Old Experiments: Deviations up to 15%



Extracted moments of the proton charge density

- **Novel method** for the **determination of the moments** of the charge density via **integral forms of the electric form factor**.
- **Reanalysis** of some **GE experimental data (Rosenbluth + low k^2)**
 - Extraction of **several moments of the charge density taking all error sources** into consideration
- **Necessity to have experimental data at low k^2** for a better determination of high order positive moments (large-distance effects)
- **Importance to have data at high k^2** necessary in the evaluation of negative order moments (short-distance effects)
- Extend the application to include measurements of $G_M(k^2) + \frac{\mu G_E(k^2)}{G_M(k^2)}$ and access **magnetic moments** as well as **Zemach moments**

λ	$\langle r^\lambda \rangle_Q$ [fm $^\lambda$]	$\langle r^\lambda \rangle$ [fm $^\lambda$]	Stat. Error $\delta [\langle r^\lambda \rangle_Q]$ [fm $^\lambda$]	Syst. Error		
				Dat. [fm $^\lambda$]	Fun. [fm $^\lambda$]	Mod. [fm $^\lambda$]
-2	6.5826	8.9093	0.0039	0.0141	0.0008	0.0183
-1	1.9752	2.1043	0.0005	0.0024	0.0002	0.0022
1	0.7186	0.7158	0.0004	0.0025	0.0001	0.0008
2	0.6824	0.6824	0.0020	0.0113	0.0001	0.0053
3	0.7966	0.7970	0.0096	0.0500	0.0005	0.0300
4	1.0208	1.0208	0.0515	0.2498	0.0042	0.1752
5	0.9219	0.9217	0.3098	1.4388	0.0273	1.0995
6	-3.6823	-3.6823	2.0835	9.5186	0.2372	7.5914
7	-49.6804	-49.6802	15.8544	71.544	1.7403	58.198

Systematic errors related to **experimental data of FF**

Bias that could be generated from the **fit function**

Errors attached to the **choice of the fitting model**



DVCS on proton and neutron from a deuterium target

- Work in collaboration with Silvia Niccolai for the CLAS collaboration

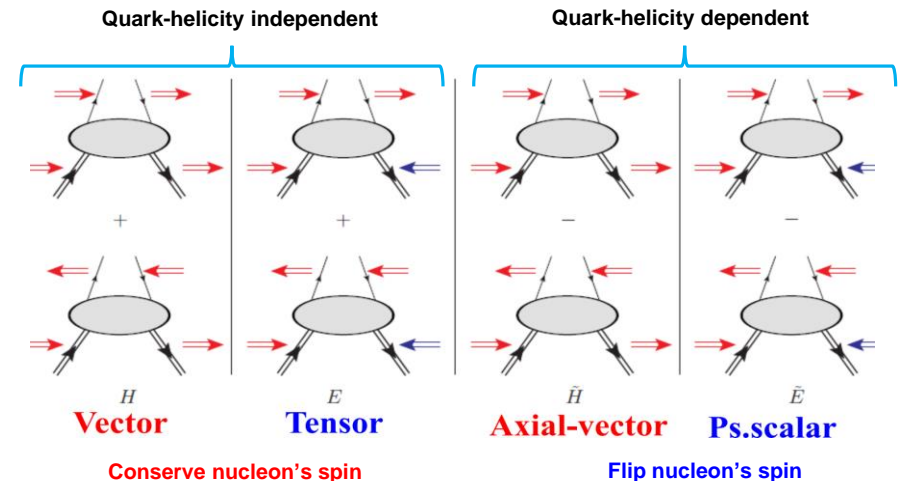
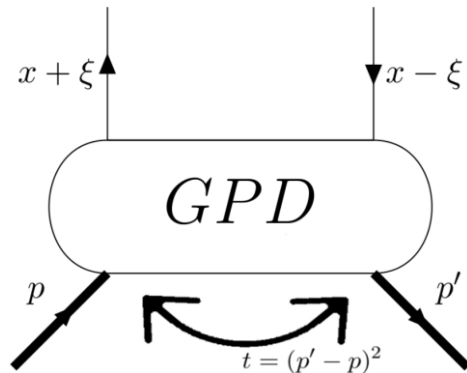
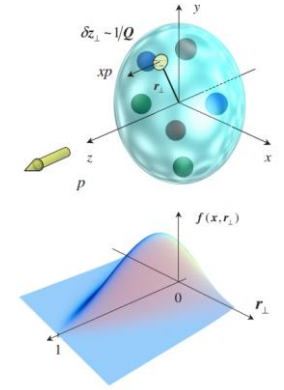


- QCD at low energies: non perturbative regime
 - Need **structure functions** to describe nucleon structure

GPDs

Correlation of transverse position and longitudinal momentum of partons in the nucleon & the spin structure - through Ji's sum rule X. Ji, Phy.Rev.Lett.78,610(1997)

- GPDs can be accessed through **exclusive leptonproduction reactions**
- At leading order QCD, chiral-even (quark helicity is conserved), quark sector: 4 **GPDs** for each quark flavor H, \tilde{H}, E and \tilde{E}
- GPDs depend on x, ξ and $t = (p' - p)^2$





Why are GPDs important?

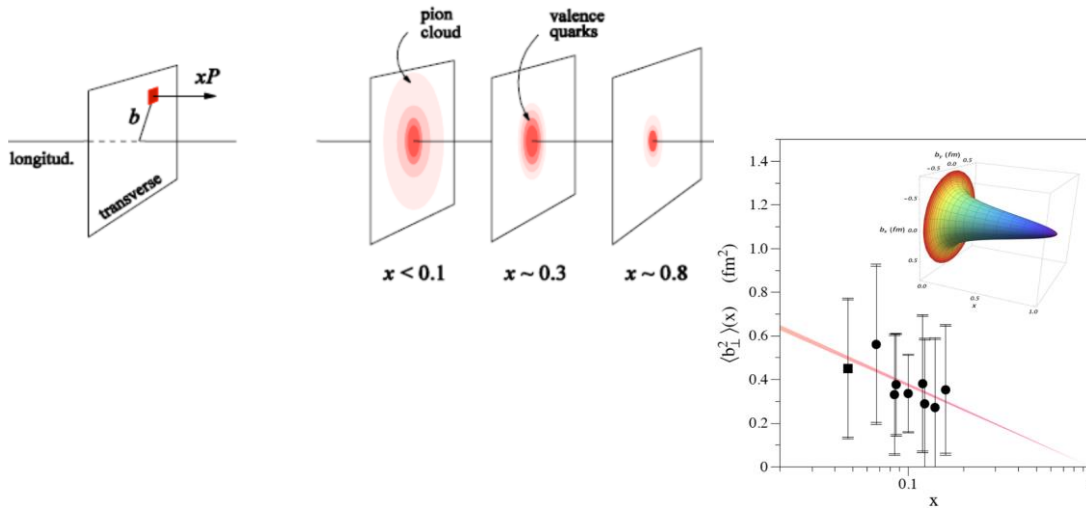
- GPDs: Fourier transforms of non-local, non-diagonal QCD operators

Nucleon tomography

M. Burkardt, PRD 62, 71503 (2000)

$$q(x, b_{\perp}) = \int_0^{\infty} \frac{d^2 \Delta_{\perp}}{(2\pi)^2} e^{i\Delta_{\perp} b_{\perp}} H(x, 0, -\Delta_{\perp}^2)$$

$$\Delta q(x, b_{\perp}) = \int_0^{\infty} \frac{d^2 \Delta_{\perp}}{(2\pi)^2} e^{i\Delta_{\perp} b_{\perp}} \tilde{H}(x, 0, -\Delta_{\perp}^2)$$



R. Dupré, M. Guidal, M. Vanderhaeghen, PRD95, 011501 (2017)

Quark angular momentum

X. Ji, Phys.Rev.Lett.78,610(1997)

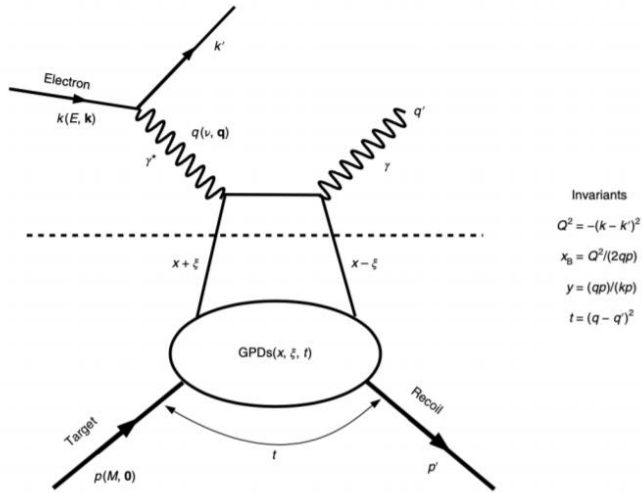
$$\frac{1}{2} \int_{-1}^1 x dx (H(x, \xi, t=0) + E(x, \xi, t=0)) = J = \frac{1}{2} \Delta\Sigma + \Delta L$$

$$\text{Nucleon spin: } \frac{1}{2} = \frac{1}{2} \Delta\Sigma + \Delta L + \Delta G$$

- The intrinsic spin of the quarks can not explain the origin of the spin of the nucleon (**nucleon Spin Crisis**)
- Intrinsic spin of the gluons
- GPDs: quantify the contribution of orbital angular momentum of quarks to the nucleon spin



Deeply Virtual Compton Scattering of leptons off nucleons



- DVCS allows access to 4 complex GPDs-related quantities:
 - Compton Form Factors (x, ξ, t) (CFFs)

$$\mathcal{H} = \sum_q e_q^2 \left\{ i \pi [H^q(\xi, \xi, t) - H^q(-\xi, \xi, t)] + \mathcal{P} \int_{-1}^1 dx H^q(x, \xi, t) \left[\frac{1}{\xi - x} - \frac{1}{\xi + x} \right] \right\}$$

- x can not be accessed experimentally by DVCS: Models needed to map the x dependence

$$\sigma(eN \rightarrow eN\gamma) = \left[\text{DVCS} + \text{Bethe-Heitler (BH)} \right]^2$$

BH is purely electromagnetic and parametrised by FFs

- Experimentally measured observables:
 - Sensitive to the DVCS-BH interference part (linear in CFFs)
 - Should have: Beam polarized and/or target polarized
 - Access to a combinations of CFFs
 - The separation of CFFs requires the measurement of several observables
 - Depending on the target (proton or neutron): different sensitivity to the CFFs (GPDs)
 - The flavor separation of GPDs requires measurements on both nucleons

$$(H, E)_u(\xi, \xi, t) = \frac{9}{15} [4(H, E)_p(\xi, \xi, t) - (H, E)_n(\xi, \xi, t)]$$

$$(H, E)_d(\xi, \xi, t) = \frac{9}{15} [4(H, E)_n(\xi, \xi, t) - (H, E)_p(\xi, \xi, t)]$$



Different contributions from F_1 and F_2 for the different nucleons

Polarized beam, unpolarized target

$$\Delta\sigma_{LU} \sim \sin(\phi) \Im\{F_1 \mathbf{H} + \xi(F_1 + F_2) \tilde{\mathbf{H}} - k F_2 \mathbf{E} + \dots\}$$

Unpolarized beam, polarized target

$$\Delta\sigma_{UL} \sim \sin(\phi) \Im\left\{F_1 \tilde{\mathbf{H}} + \xi(F_1 + F_2) \left(\mathbf{H} + \frac{x_b}{2} \mathbf{E}\right) - \xi k F_2 \tilde{\mathbf{E}}\right\}$$

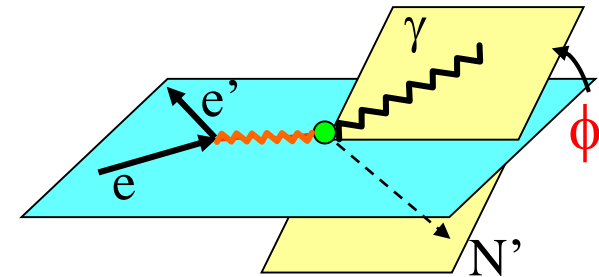
polarized beam, longitudinal polarized target

$$\Delta\sigma_{LL} \sim (A + B \cos(\phi)) \Re\{F_1 \tilde{\mathbf{H}} + \xi(F_1 + F_2) \left(\mathbf{H} + \frac{x_b}{2} \mathbf{E}\right) + \dots\}$$

unpolarized beam, transverse polarized target

$$\Delta\sigma_{UT} \sim \cos(\phi) \sin(\phi_s - \phi) \Im\{k(F_2 \mathbf{H} - F_1 \mathbf{E}) + \dots\}$$

Observable	Proton	Neutron
$\Delta\sigma_{LU}$	$\Im\{\mathbf{H}_p, \tilde{\mathbf{H}}_p, \mathbf{E}_p\}$	$\Im\{H_n, \tilde{H}_n, \mathbf{E}_n\}$
$\Delta\sigma_{UL}$	$\Im\{\mathbf{H}_p, \tilde{\mathbf{H}}_p\}$	$\Im\{\mathbf{H}_n, E_n\}$
$\Delta\sigma_{LL}$	$\Re\{\mathbf{H}_p, \tilde{\mathbf{H}}_p\}$	$\Re\{\mathbf{H}_n, E_n\}$
$\Delta\sigma_{UT}$	$\Im\{\mathbf{H}_p, \mathbf{E}_p\}$	$\Im\{\mathbf{H}_n\}$





Different contributions from F_1 and F_2 for the different nucleons

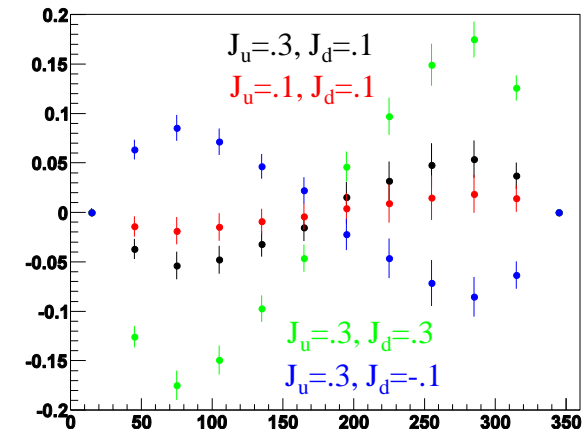
- **DVCS with an unpolarized deuterium target :**
- Scattering off neutron (nDVCS): GPD **E**
 - Determination of Ji sum rule
 - Contribution of orbital angular momentum of quarks to the nucleon spin

$$\frac{1}{2} \int_{-1}^1 x dx (H(x, \xi, t=0) + E(x, \xi, t=0)) = J = \frac{1}{2} \Delta \Sigma + \Delta L$$

- Scattering off proton (pDVCS): GPD **H**
 - Quantify medium effects
 - Essential for the extraction of BSA of a “free” neutron (deconvoluting medium effect via comparison with DVCS on hydrogen target)
- The BSA for nDVCS:
 - is complementary to the TSA for pDVCS on transverse target, aiming at E
 - depends strongly on the kinematics \rightarrow wide coverage needed
 - is smaller than for pDVCS \rightarrow more beam time needed to achieve reasonable statistics

Observable	Proton	Neutron
$\Delta\sigma_{LU}$	$\Im\{\mathbf{H}_p, \tilde{\mathbf{H}}_p, E_p\}$	$\Im\{H_n, \tilde{H}_n, E_n\}$
$\Delta\sigma_{UL}$	$\Im\{\mathbf{H}_p, \tilde{\mathbf{H}}_p\}$	$\Im\{\mathbf{H}_n, E_n\}$
$\Delta\sigma_{LL}$	$\Re\{\mathbf{H}_p, \tilde{\mathbf{H}}_p\}$	$\Re\{\mathbf{H}_n, E_n\}$
$\Delta\sigma_{UT}$	$\Im\{\mathbf{H}_p, E_p\}$	$\Im\{\mathbf{H}_n\}$

Model predictions (VGG) for different values of quarks' angular momentum



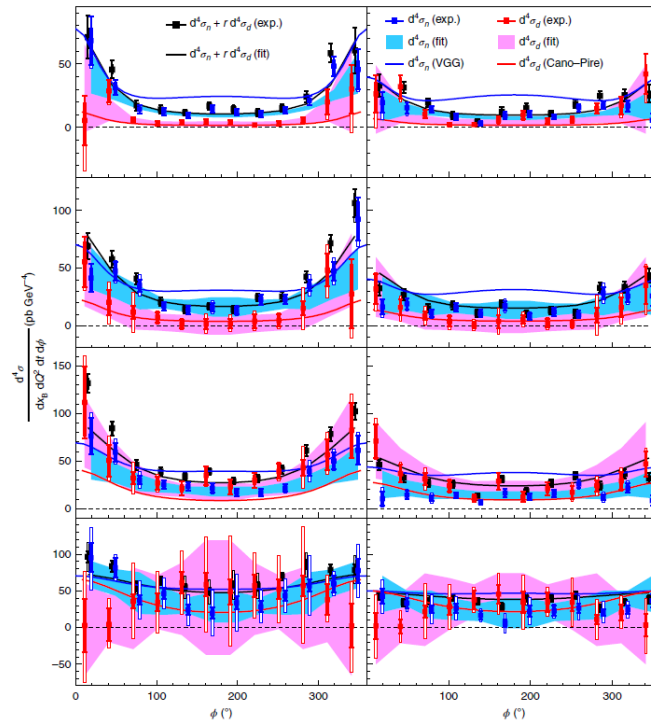


Deeply Virtual Compton Scattering with an unpolarized deuterium target

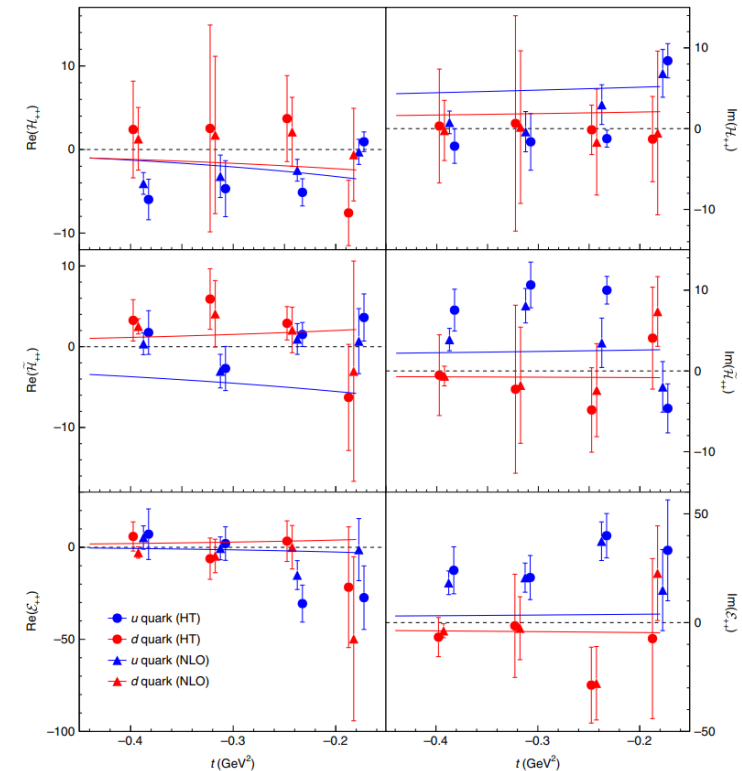
- Previous pioneering measurement of nDVCS (Jlab Hall A @ 6 GeV)
 - Beam-energy « Rosenbluth » separation of nDVCS CS using an LD2 target and two different beam energies
 - First observation of non-zero nDVCS CS

• No neutron detection $D(e, e'\gamma)X - H(e, e'\gamma)X = n(e, e'\gamma)n + d(e, e'\gamma)d + \dots$

One measured kinematical point:
 $Q^2=1.9 \text{ GeV}^2$ and $x_B=0.36$



+data from: Mazouz, M. et al. Phys. Rev. Lett. 99, 242501 (2007).



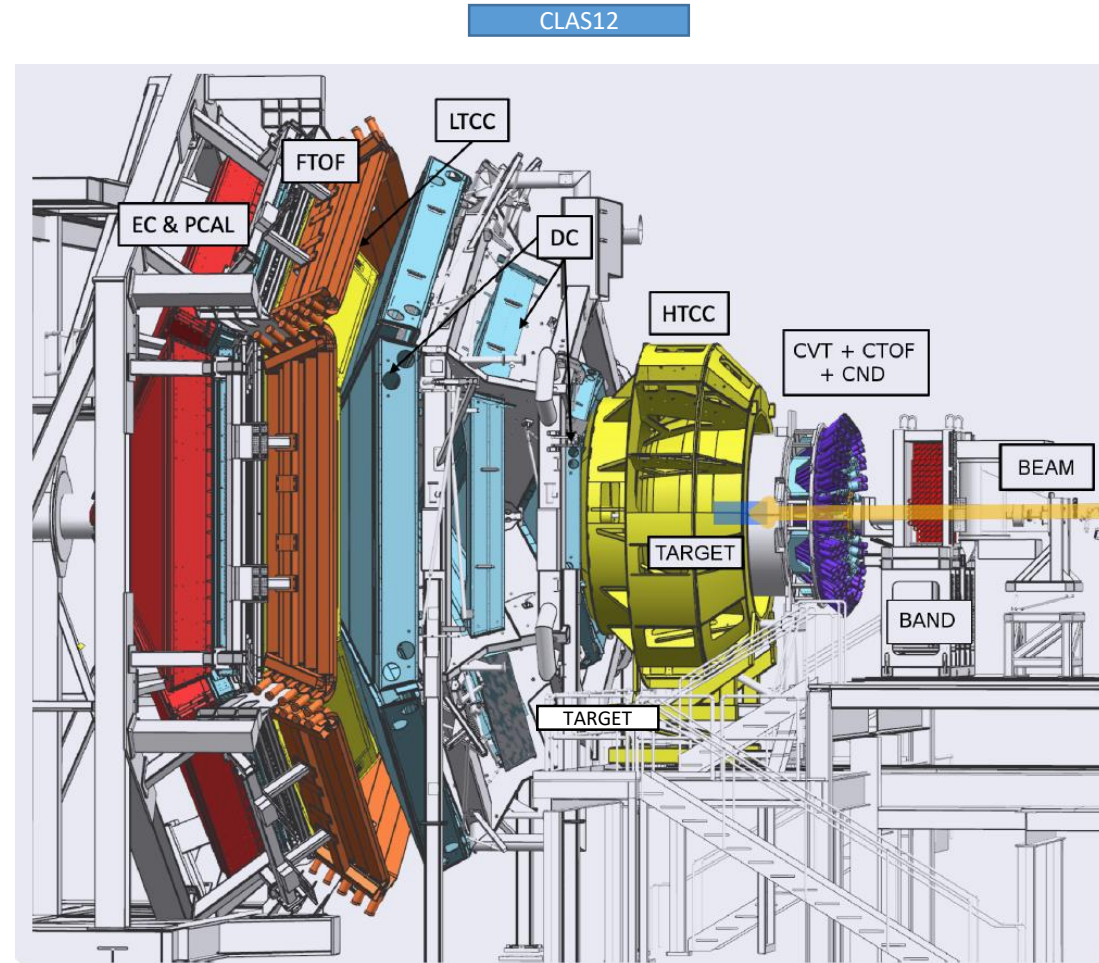
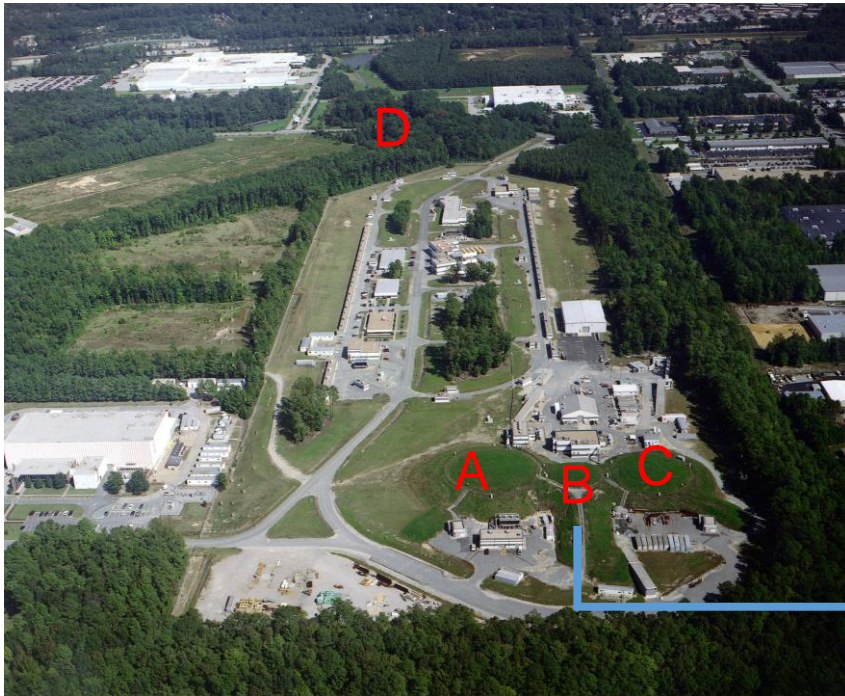
Benali, M., Desnault, C., Mazouz, M. et al. Nat. Phys. 16, 191–198 (2020)



The CEBAF and CLAS at Jefferson Laboratory

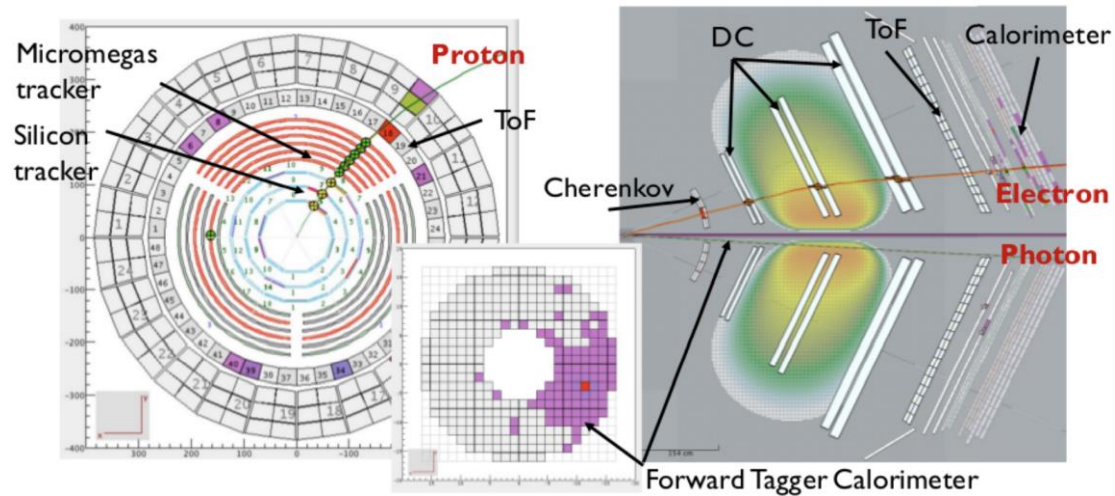
Continuous Electron Beam Accelerator Facility

- Up to 12 GeV electrons
- Two anti-parallel linacs, with recirculating arcs on both ends
- 4 experimental halls



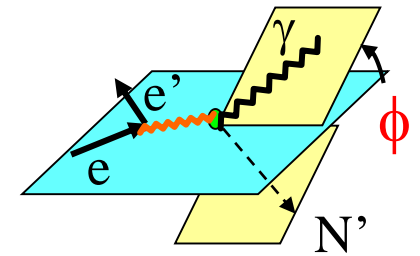
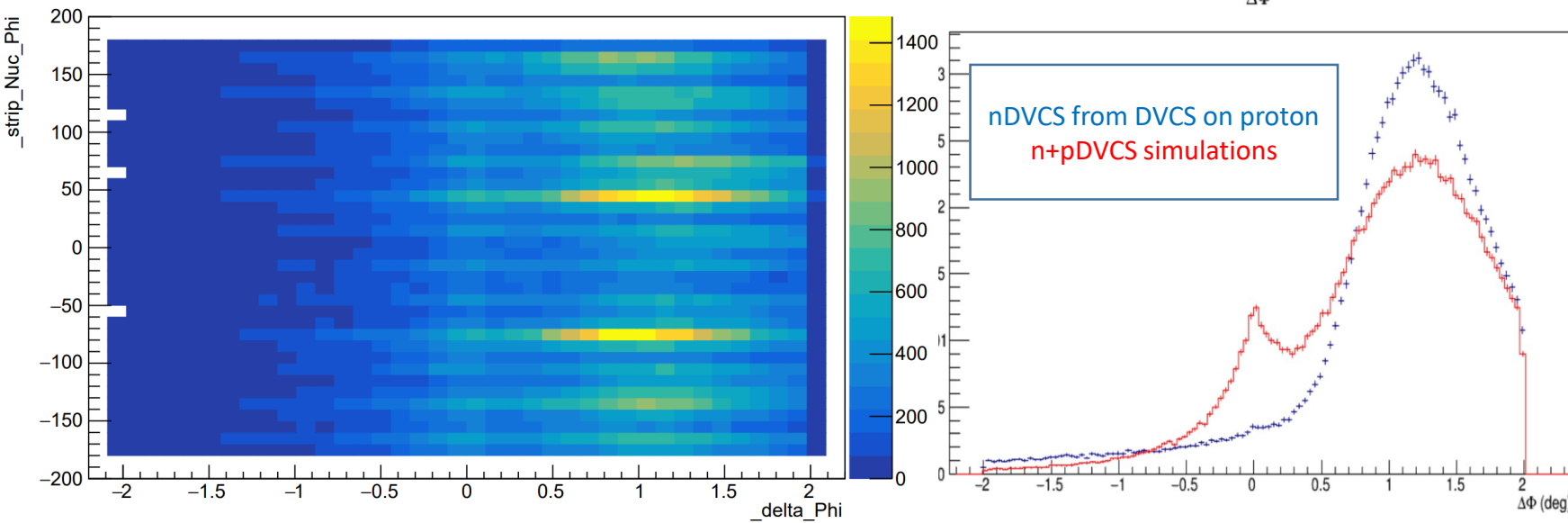


- A 10.6/10.4/10.2 GeV electron beam
 - With an average polarization of 86%
 - Scattering off an unpolarized Liquid Deuterium target of 5 cm length
- The exclusivity of the event is insured by:
 - **Electron detection**: Cerenkov detector, drift chambers and electromagnetic calorimeter
 - **Photon detection**: sampling calorimeter or a small PbWO₄-calorimeter close to the beamline
 - **Proton detection**: Silicon and Micromegas detector OR **Neutron detection**: Central Neutron Detector
- For Neutron Detection:
 - Machine Learning techniques are applied to improve the Identification and reduce charged particle contamination





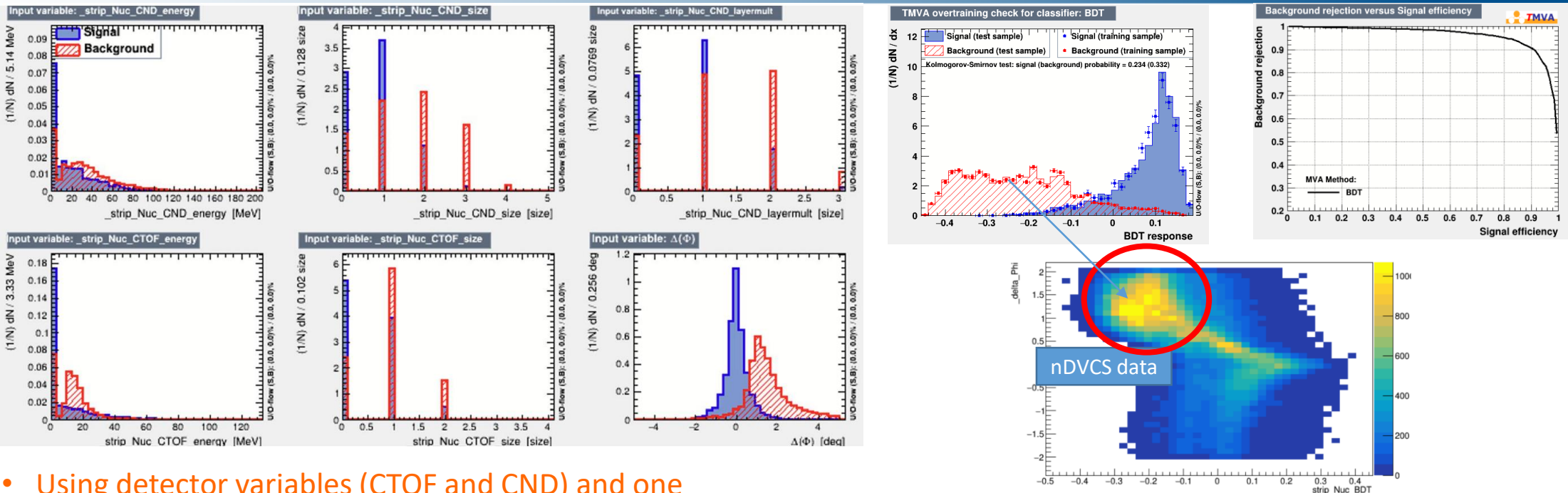
- The tracking of the CVT is neither 100% efficient nor uniform
- In the dead regions of the CVT **protons** have no associated track and thus can be **misidentified as neutrons**
- Protons roughly account for more than **>40% contamination in the “nDVCS”** signal sample Current approach, based on Machine Learning & Multi-Variate Algorithms:
 - We reconstruct nDVCS from DVCS experiment on proton requiring neutron PID : **selected neutron are misidentified protons**
 - We use this sample to determine the characteristics of fake neutrons in low- and high-level reconstructed variables
 - Based on those characteristics we subtract the fake neutrons contamination from nDVCS
 - As a « signal » sample in the training of the ML we use $ep \rightarrow en\pi^+$ events from DVCS experiment on proton



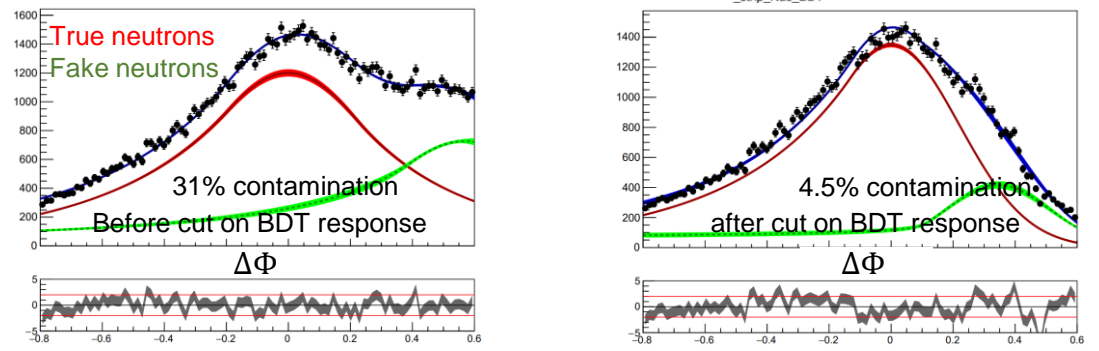


Improving the neutron selection with ML techniques

Under internal review

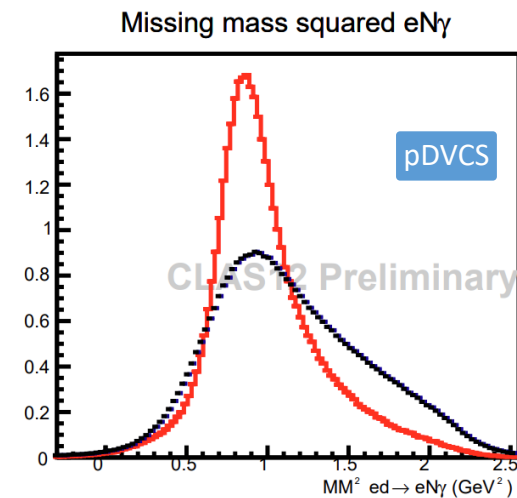
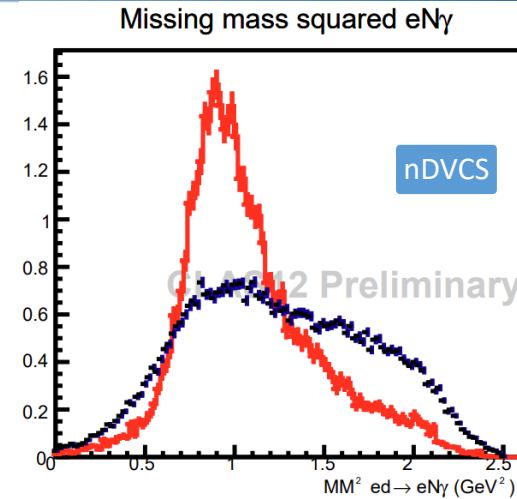


- Using detector variables (CTOF and CND) and one exclusivity variable ($\Delta\Phi$)
- Directly trained on data
- Better optimization of signal to background ratio than straight cuts
- Few percent irreducible contamination is to be taken as a systematic on the BSA





- The nDVCS (pDVCS) final state is selected with the following exclusivity criteria: (N:nucleon)
 - Missing mass
 - $e d \rightarrow e N \gamma X$
 - $e N \rightarrow e N \gamma X$
 - $e N \rightarrow e N X$
 - Missing momentum
 - $e d \rightarrow e N \gamma X$
 - $\Delta\Phi, \Delta t, \theta(\gamma, X)$
 - Difference between two ways of calculating Φ and t
 - Cone angle between measured and reconstructed photon
- Exclusivity selection is optimized with a 4-D χ^2 -like distribution including $\Delta\Phi, \Delta t, \theta(\gamma, X)$ and missing mass $e N \rightarrow e N X$



π^0 background contamination is estimated using simulations



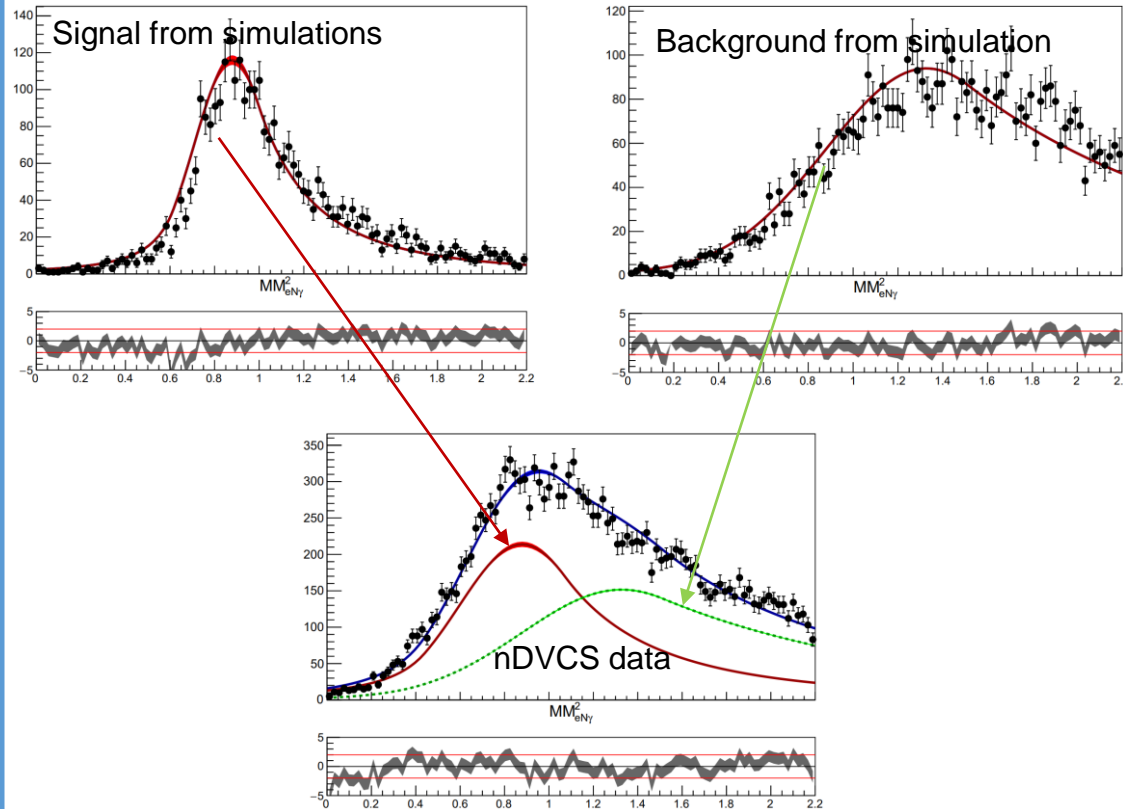
- Subtraction using simulations of the background channel
 - Monte Carlo simulations:
 - GPD-based event generator for DVCS/ π^0 on deuterium
 - DVCS amplitude calculated according to the BKM formalism
 - Fermi-motion distribution evaluated according to Paris potential
- Estimate the ratio of partially reconstructed $eN \pi^0(1 \text{ photon})$ decay to fully reconstructed $eN \pi^0$ decays in MC
 - This is done for each kinematic bin to minimize MC model dependence
 - Multiply this ratio by the number of reconstructed $eN \pi^0$ in data to get the number of $eN \pi^0(1 \text{ photon})$ in data
 - Subtract this number from DVCS reconstructed decays in data per each kinematical bin

$$\text{Simulations: } R = \frac{N(eN\pi_{1\gamma}^0)}{N(eN\pi^0)}$$

$$\text{Data: } N(eN\pi_{1\gamma}^0) = R * N(eN\pi^0)$$

$$N(DVCS) = N(DVCS_{recon}) - N(eN\pi_{1\gamma}^0)$$

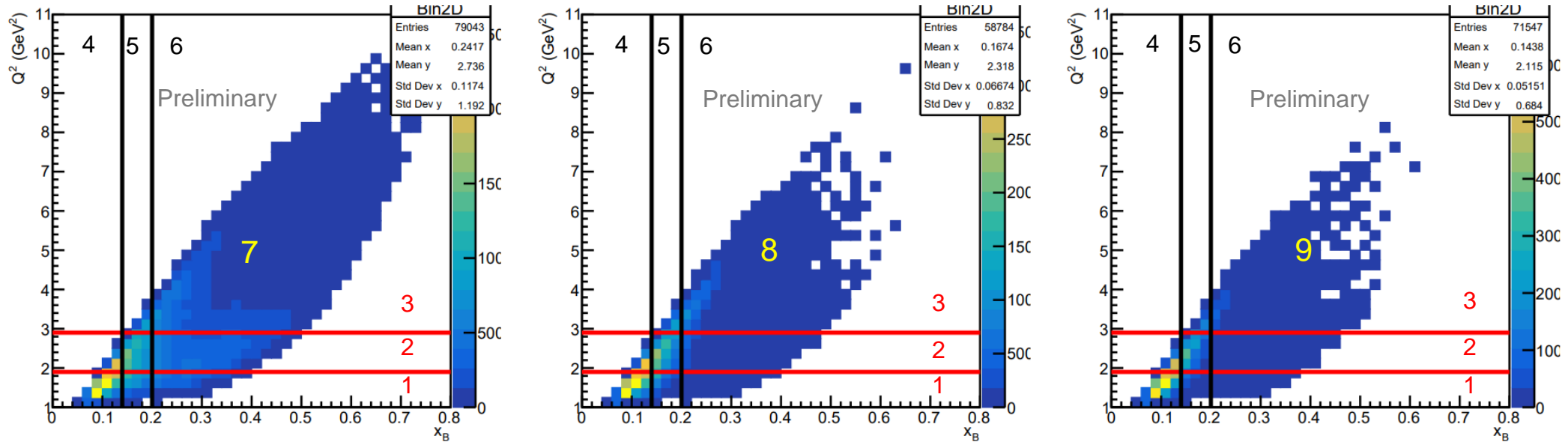
- π^0 background subtraction is also performed by statistical unfolding of contribution to the missing mass spectrum
M. Pivk and F.R. Le Diberder, NIMA 555 1 2005



The difference between the estimations of background from both methods is considered as a systematic



First-time measurement of nDVCS with detection of the active neutron

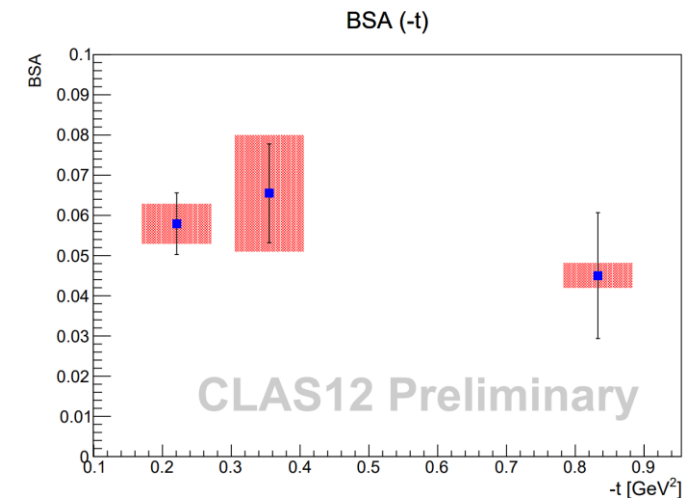
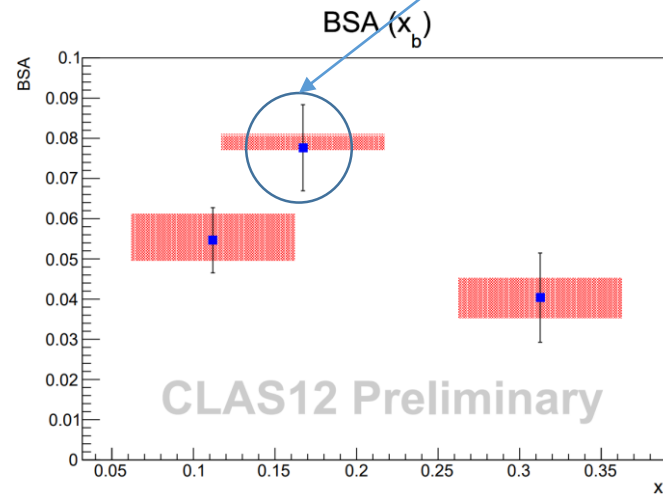
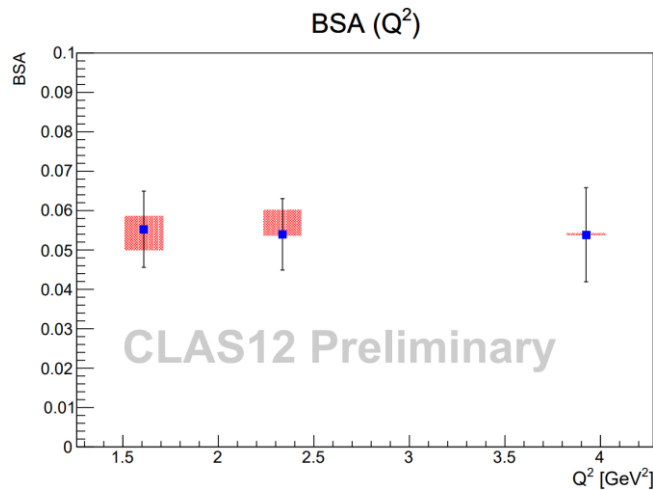
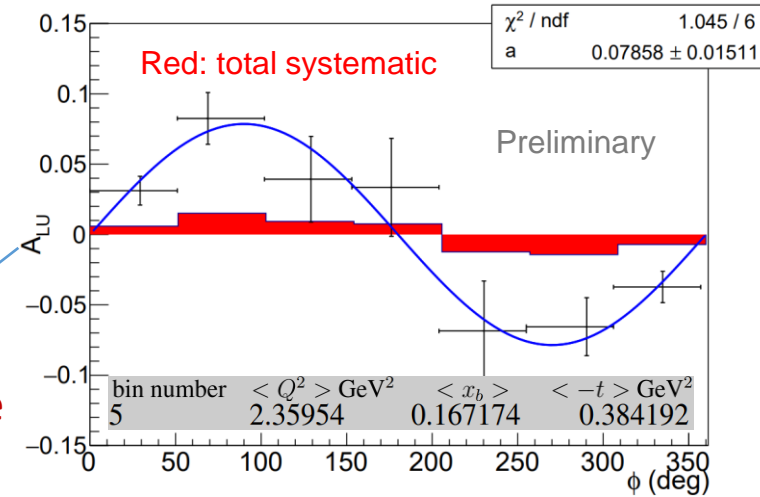


bin number	$\langle Q^2 \rangle$ GeV ²	$\langle x_b \rangle$	$\langle -t \rangle$ GeV ²
1	1.60973	0.132015	0.388061
2	2.33568	0.199322	0.467386
3	3.92472	0.314797	0.667296
4	1.70901	0.111932	0.324567
5	2.35954	0.167174	0.384192
6	3.29066	0.312552	0.70405
7	2.91918	0.277885	0.832902
8	2.44265	0.185242	0.355265
9	2.16854	0.149355	0.22063

- Compared to the previous experiment, CLAS12 provides :
 - The possibility to scan the BSA of nDVCS on a wide phase space
 - The possibility to reach the high Q^2 high x_b region of the phase space
 - Exclusive measurement with the detection of the active neutron
- Hall A @ JLAB: one measured kinematical point at $Q^2=1.9$ GeV² and $x_b=0.36$

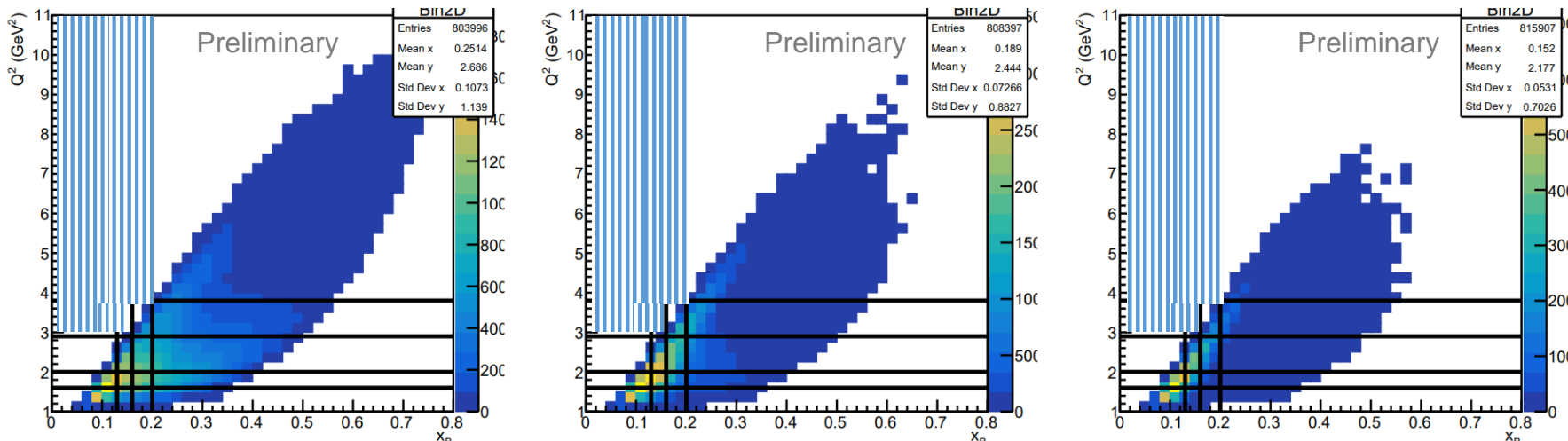


- Observation of positive BSA for nDVCS
- Systematic errors include:
 - Error due to beam polarization
 - Error due to selection cuts
 - Error due to residual proton contamination
 - Error due to merging of data sets with different energies
- Statistics is expected to double with remaining scheduled beam time and improvements with reconstruction software





First-time measurement of incoherent pDVCS on deuteron



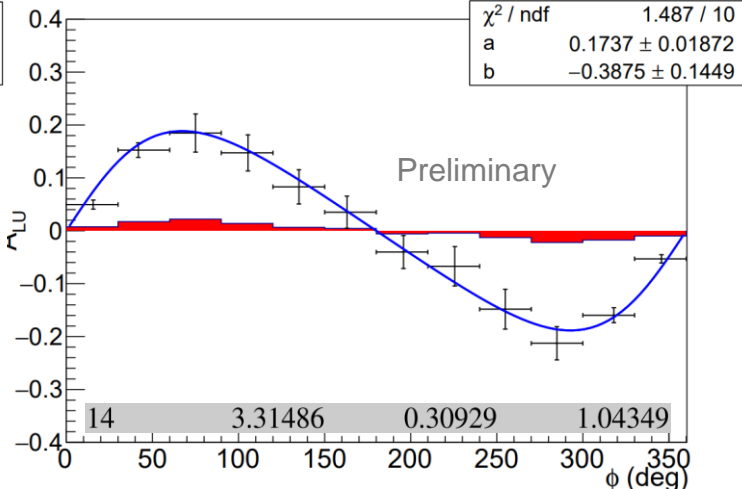
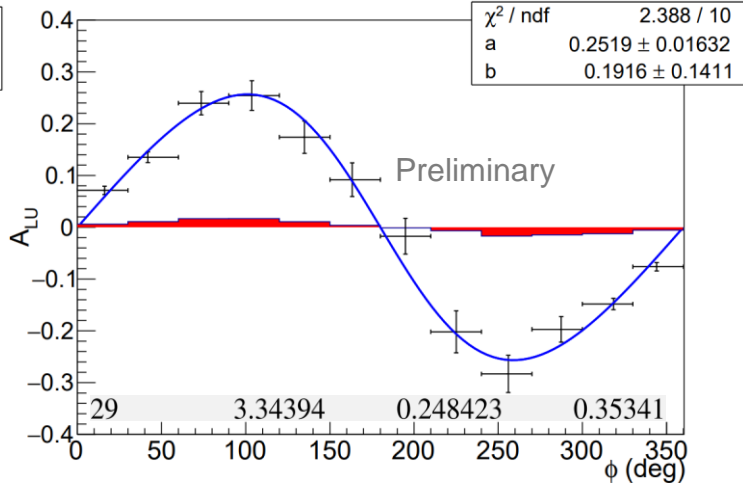
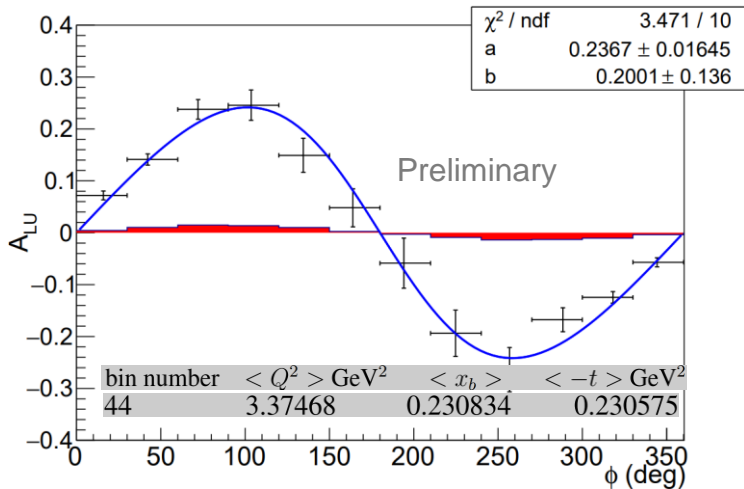
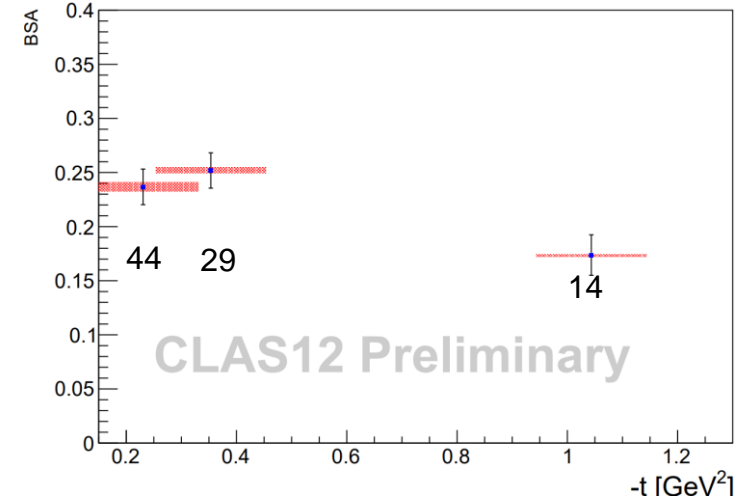
Bin numbering starts from left to right and from bottom up

- Complementary to previous experiment on proton target:
 - Quantify medium effects on GPDs

bin number	$\langle Q^2 \rangle$ GeV ²	$\langle x_b \rangle$	$\langle -t \rangle$ GeV ²
1	1.43794	0.10069	0.767361
2	1.48186	0.144366	0.844629
3	1.4914	0.178824	0.87073
4	1.50756	0.2373	0.851789
5	1.76792	0.114657	0.777427
6	1.8051	0.144373	0.825599
7	1.80447	0.179402	0.863781
8	1.81536	0.258406	0.923301
9	2.0849	0.124705	0.764681
10	2.26532	0.146577	0.793068
11	2.4122	0.179697	0.827414
12	2.43479	0.287563	1.00085
13	3.0799	0.188297	0.790217
14	3.31486	0.30929	1.04349
15	4.83889	0.380624	1.228
16	1.43915	0.100179	0.356721
17	1.49262	0.142616	0.362959
18	1.4954	0.176071	0.350067
19	1.50509	0.249393	0.309281
20	1.77057	0.114679	0.34701
21	1.81394	0.143668	0.348841
22	1.82669	0.175209	0.355866
23	1.81383	0.263491	0.318227
24	2.08646	0.124711	0.342502
25	2.26728	0.146758	0.340636
26	2.46209	0.17752	0.348786
27	2.45997	0.26518	0.340427
28	3.08043	0.188274	0.334151
29	3.34394	0.248423	0.35341
30	4.46623	0.295696	0.370628
31	1.43626	0.0986234	0.200339
32	1.50515	0.13983	0.218898
33	1.49559	0.17749	0.195675
34	1.50618	0.241843	0.211988
35	1.77032	0.114665	0.198266
36	1.83854	0.140417	0.212787
37	1.82375	0.176723	0.20719
38	1.81611	0.248591	0.216637
39	2.08516	0.124803	0.198108
40	2.27128	0.145977	0.203877
41	2.55103	0.174046	0.21458
42	2.44112	0.256179	0.228055
43	3.07532	0.187944	0.210093
44	3.37468	0.230834	0.230575
45	4.30035	0.274016	0.247191



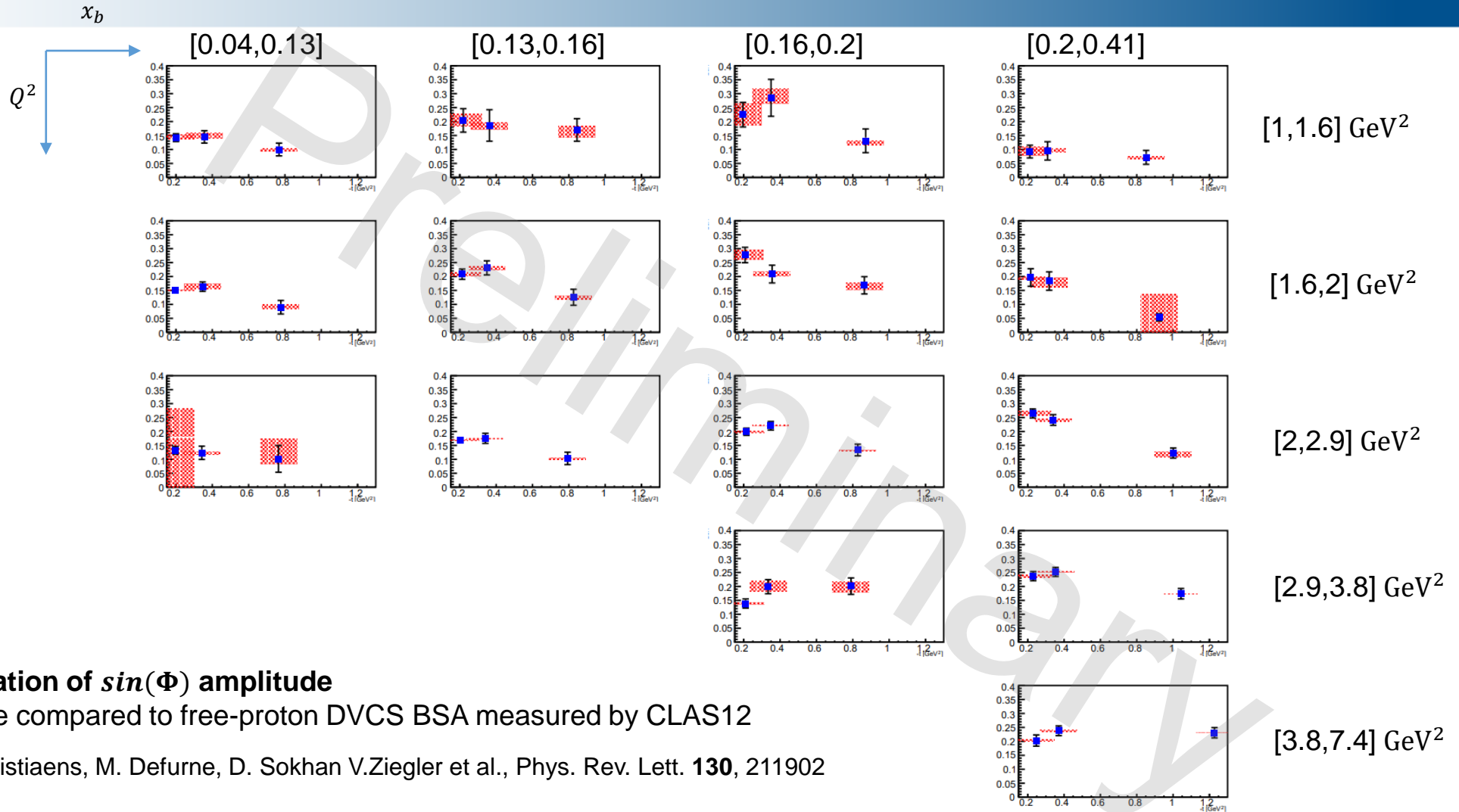
- Systematic errors include:
 - Error due to beam polarization
 - Error due to selection cuts
 - Error due to merging of data sets with different energies
- Statistics is expected to triple with remaining scheduled beam time and improvements with reconstruction software





CLAS12: pDVCS with an unpolarized deuterium target

Under internal review



Variation of $\sin(\Phi)$ amplitude

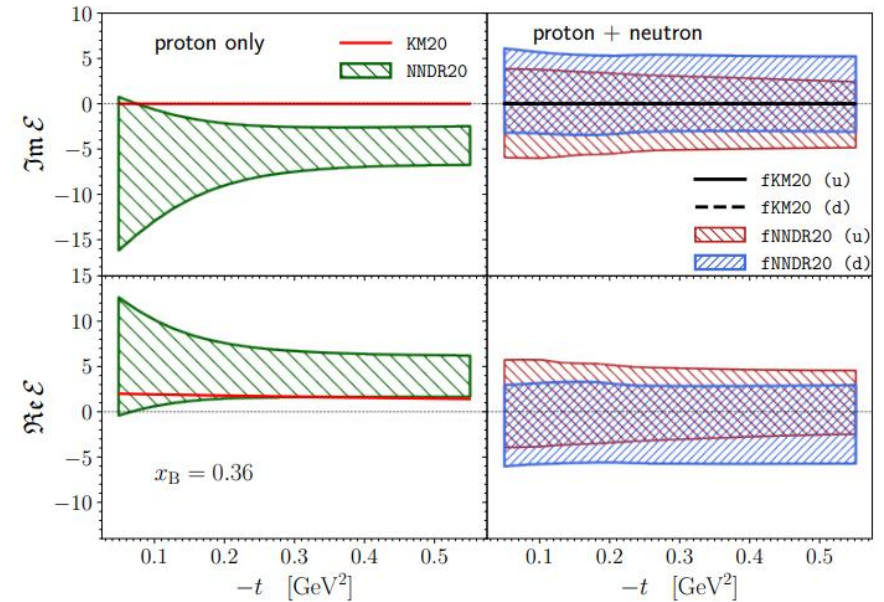
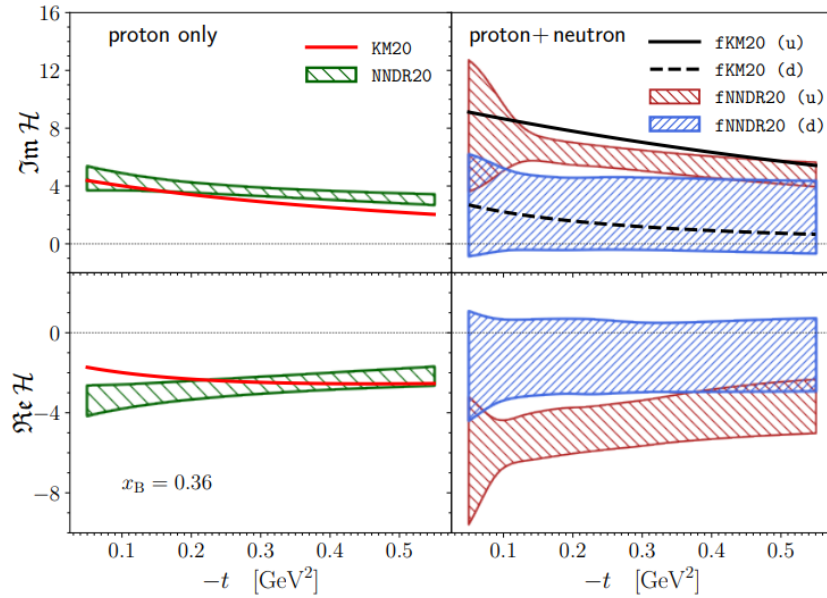
To be compared to free-proton DVCS BSA measured by CLAS12

G. Christiaens, M. Defurne, D. Sokhan V.Ziegler et al., Phys. Rev. Lett. **130**, 211902



Impact of new data

- Previous attempt at flavor separation by Marija Čuić and Krešimir Kumerički arxiv 2007.00029

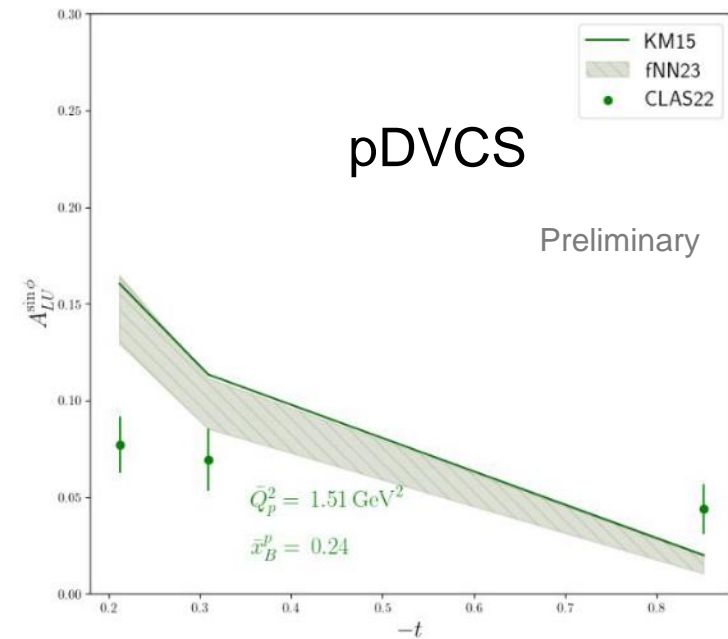
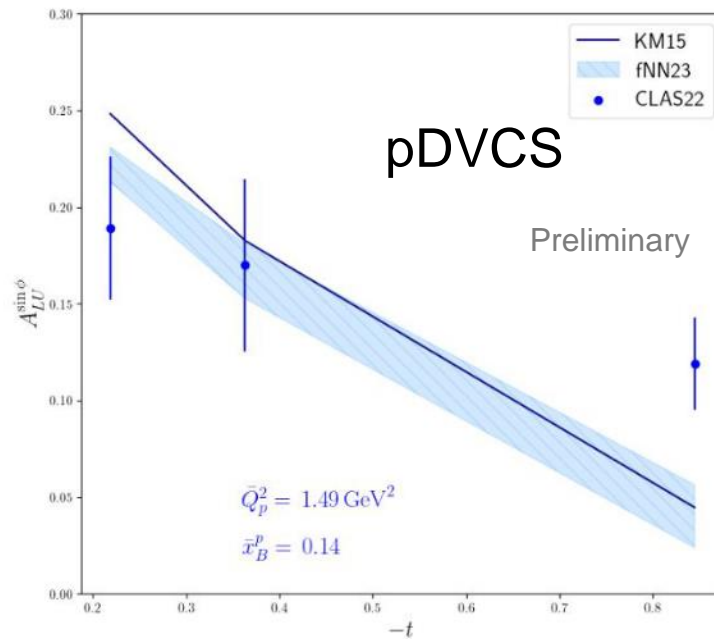
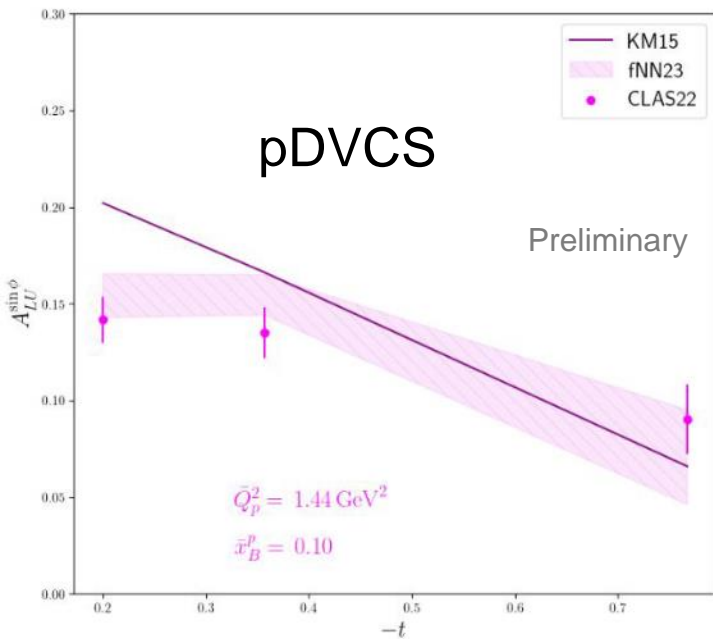


- up and down contributions to CFF H cleanly separated

- CFF E cannot be separated

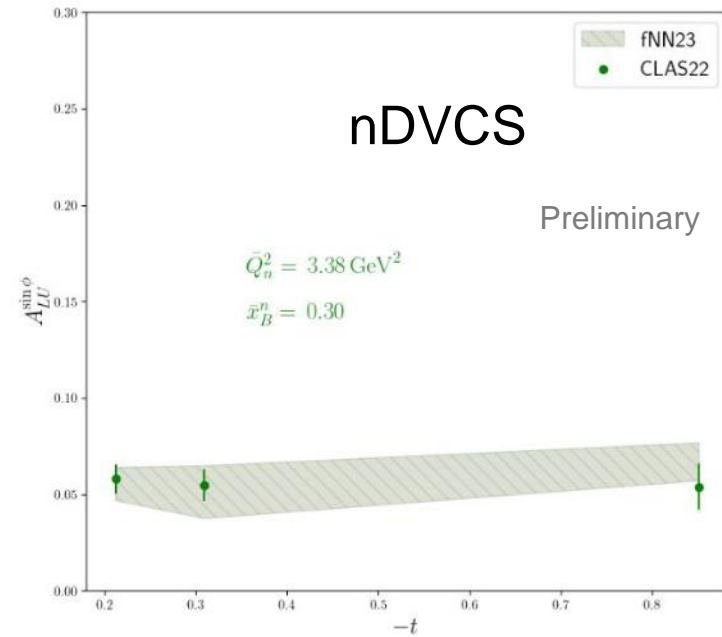
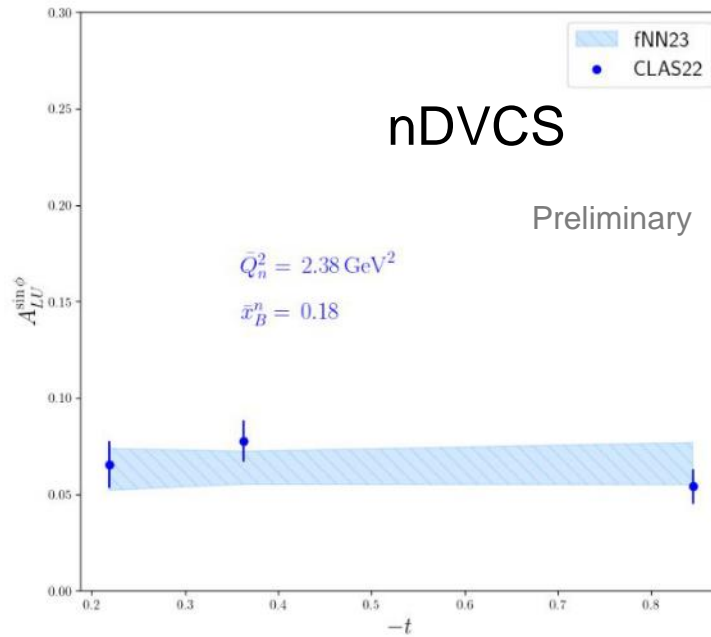
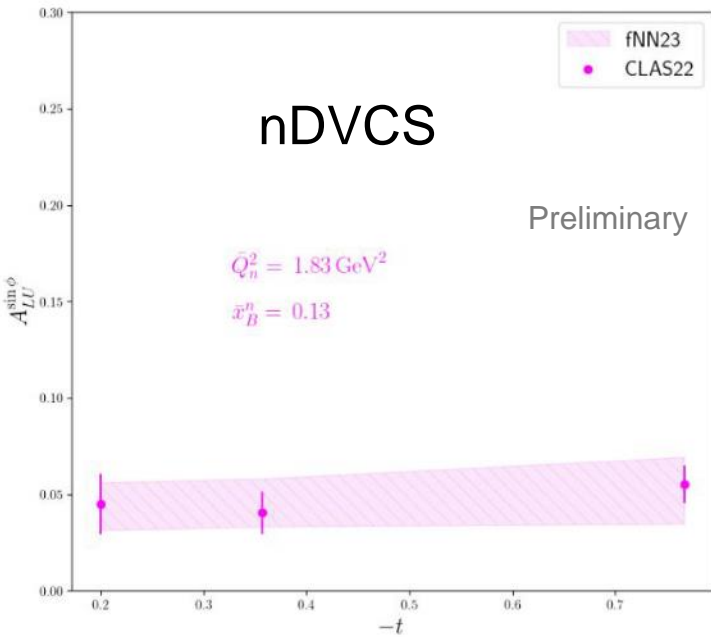


- Testing previously trained NN fits on new data was not appropriate
 - Reweighting procedure where only subset of neural nets that describes the new data well is kept in the model did not succeed
 - New data falls outside of the kinematics region of the trained models
- Solution: train new models with old CLAS6 and new CLAS12 data included in the training



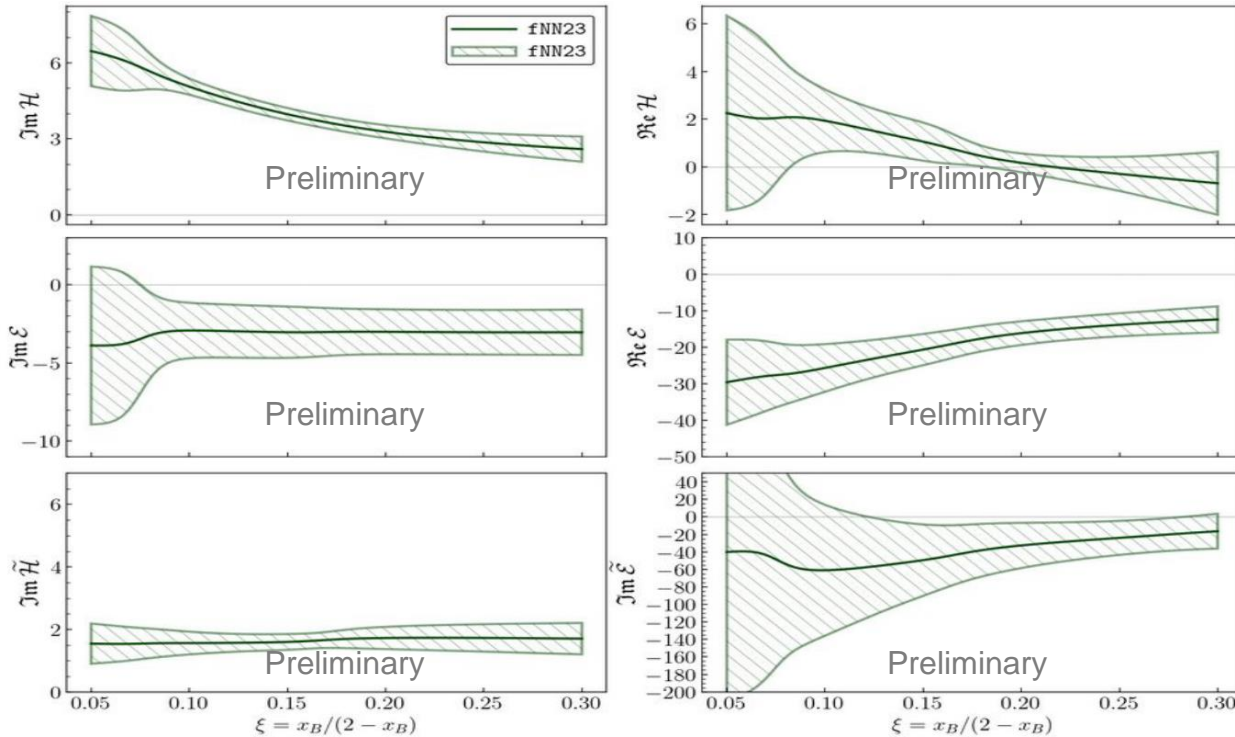


- Testing previously trained NN fits on new data was not appropriate
 - Reweighting procedure where only subset of neural nets that describes the new data well is kept in the model did not succeed
 - New data falls outside of the kinematics region of the trained models
- Solution: train new models with old CLAS6 and new CLAS12 data included in the training





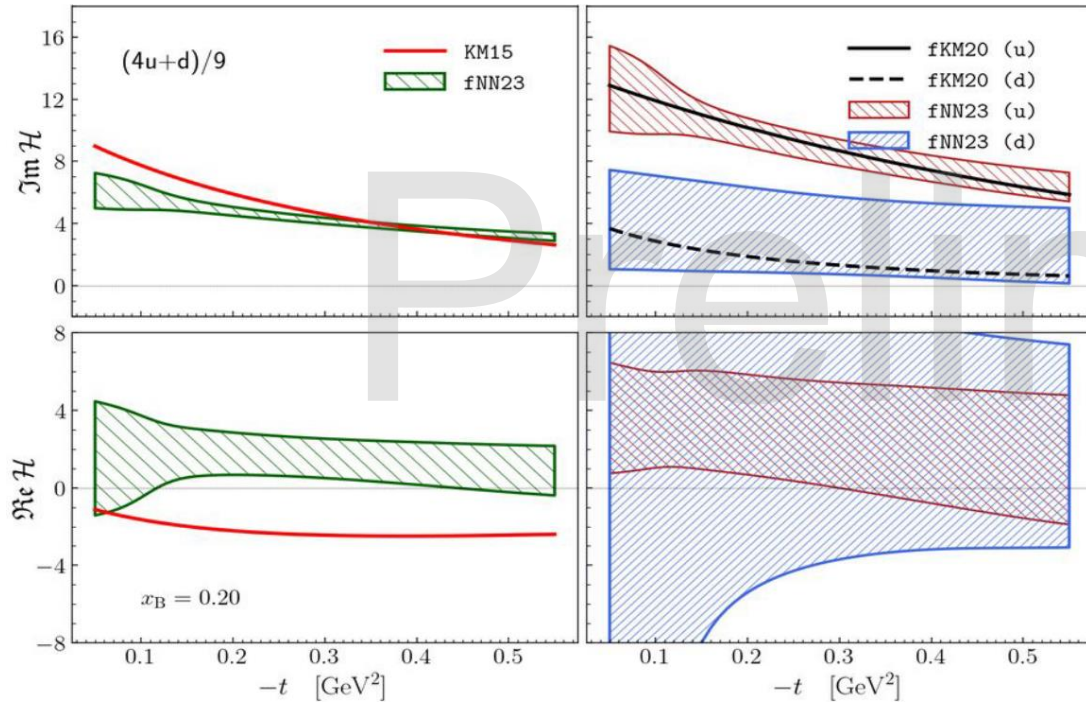
- Extraction of 6 out of 8 CFFs



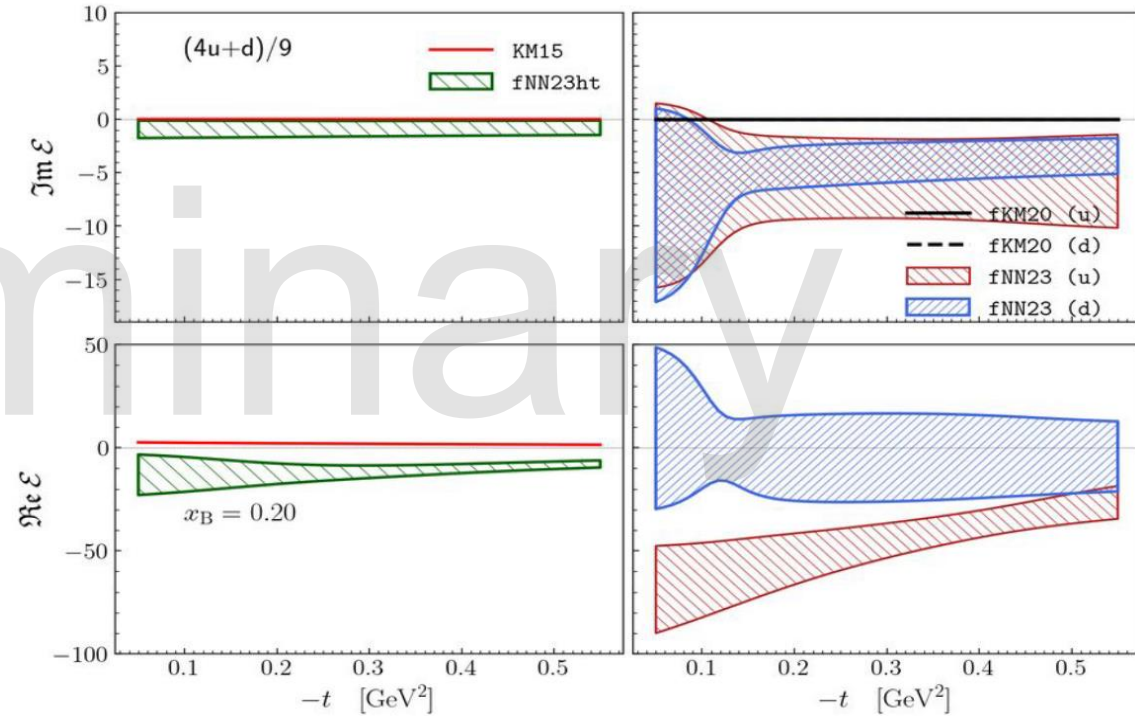
Unlike before, CFF E is now cleanly extracted, with no sign ambiguity in ReE



- Flavor separation of CFFs H and E



Flavor separation of $\text{Im}H$ is slightly better than before, while $\text{Re}H$ is worse



we can now perform flavor separation of CFF E, especially $\text{Re}E$



Summary

- GPDs are powerful tool to explore the structure of the nucleons and nuclei
 - Nucleon tomography, quark angular momentum, distribution of forces in the nucleon
- Exclusive reactions can provide important information on nucleon structure
 - DVCS via the extraction of GPDs
- CLAS12 offers a wide kinematical reach over which the GPDs dependence on different kinematical variables can be scanned
 - Data to add constraints on GPDs in unexplored regions of the phase space
 - Possibilities to measure new observables using different experimental configurations
 - Flavor separation of GPDs
- Promising results from incoherent DVCS on deuteron (n and p channels) from CLAS12 data
 - First BSA measurement from neutron-DVCS with tagged neutron
 - First measurement of BSA for proton-DVCS with deuterium target
 - To be compared to free-proton DVCS BSA measured by CLAS12

G. Christiaens, M. Defurne, D. Sokhan V.Ziegler et al., arXiv (2022) 221111274.



Decomposition and **abstraction** renders the understanding of a complex system much easier, however, the true nature of the composite system might still be unresolved

In the process of **decomposition** and **abstraction** one usually arrives to the conclusion that most constructing statements of a given theory are **irrational**



Observable (target)	CFF sensitivity	Status
ITSA(p), IDSA(p)	$\Im\{\mathbf{H}_p, \tilde{\mathbf{H}}_p\}, \Re\{\mathbf{H}_p, \tilde{\mathbf{H}}_p\}$	Data taking ended
ITSA(n), IDSA(n)	$\Im\{\mathbf{H}_n\}, \Re\{\mathbf{H}_n\}$	Data taking ended
tTSA(p)	$\Im\{\mathbf{H}_p\}, \Im\{\mathbf{E}_p\},$	Experiment foreseen for ~2025

- **JLab future energy and luminosity upgrades**

- Increase the phase space in which the GPDs are to be scanned
- And more important: scan x dependence of GPDs: **Double-DVCS**
 - Full kinematics mapping of GPDs: unique direct access to GPDs at $x \neq \pm\xi$
 - Improved detection of muons

- **And with a positron beam**

- Study beam charge asymmetries

